

Supporting Information

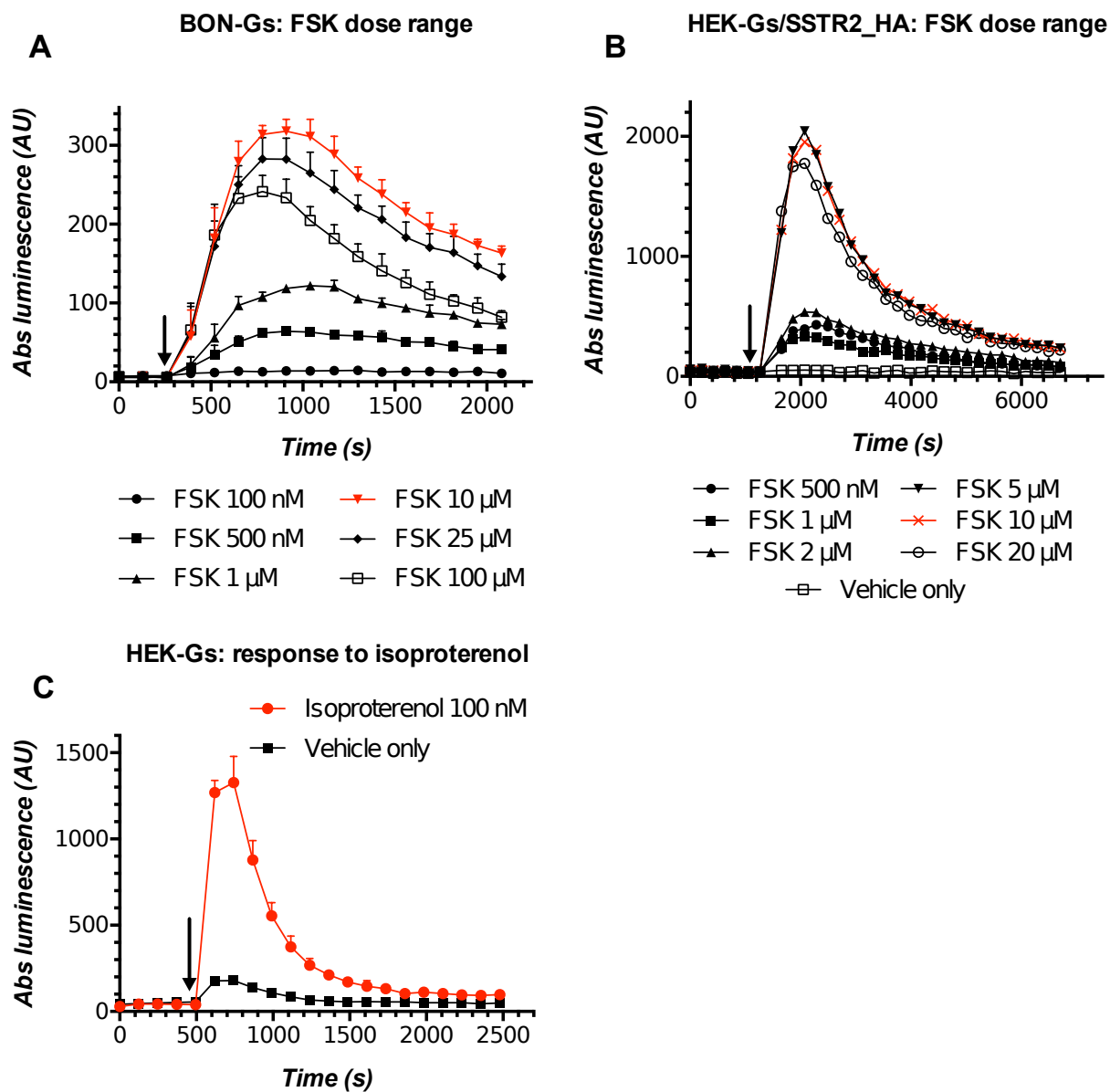
Supplementary Figure 1. The Gs22/cAMP probe registers changes in intracellular cAMP levels in living cells exposed to FSK or isoproterenol.

(A) Luminescence captured in BON-Gs cells treated with varying concentrations of FSK (100 nM – 100 μ M). The sensible stimulation of ACs, signified by a rise in cAMP and luminescence intensity, is already observable at 500 nM of FSK, with the maximum induction achieved at 10 μ M of the compound. Levels of FSK above 10 μ M produced less prominent cAMP output.

(B) A FSK dose-response study in HEK-Gs with stable overexpression of *SSTR2*. As with the BON-Gs cells, the maximum cAMP induction was achieved at about 10 μ M of FSK.

(C) Luminescence output in HEK-Gs cells exposed to 100 nM of isoproterenol. Being a non-selective agonist of β -adrenoreceptors – GPCRs that activate ACs through *G α s* subunits - isoproterenol potently induces cAMP generation, which is reflected in abrupt increase in luminescence. The small change in the signal from the control samples (treated with medium alone) is due to the bleed-through of light from the neighboring wells with the cells treated with isoproterenol and emitting strong luminescence. This effect tends to be more pronounced in assays performed in translucent plates (**panel C**) and is mitigated once the cells are placed in plates of light-tight material, e.g. 96-well ViewPlates (PerkinElmer) (**panel B**). The charts depict results of representative experiments performed in several technical replicates (in 4x, 3x and 2x – for **panels A, B and C**, respectively). The experiments were run at RT and without IBMX in the Induction Mix. Black arrow indicates the moment when compounds were added to the cells. y-axis represents absolute luminescence values (AU), x-axis denotes time scale (s). Error bars represent mean +/-

SD (with only SD's upper half shown); the curves on **panel B** are shown without error bars for visual clarity.



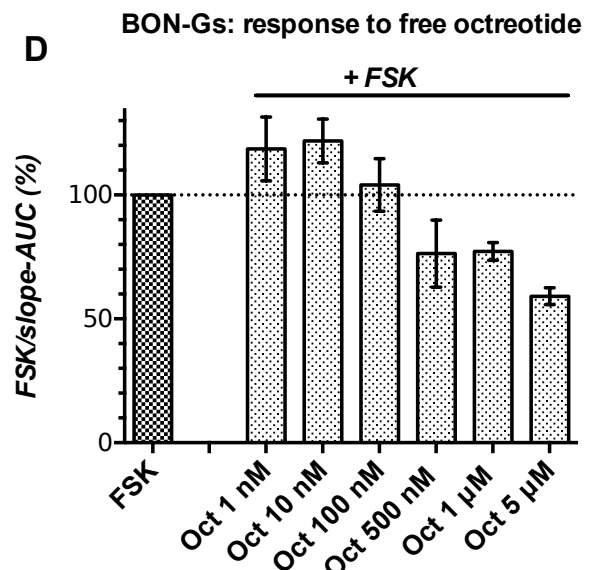
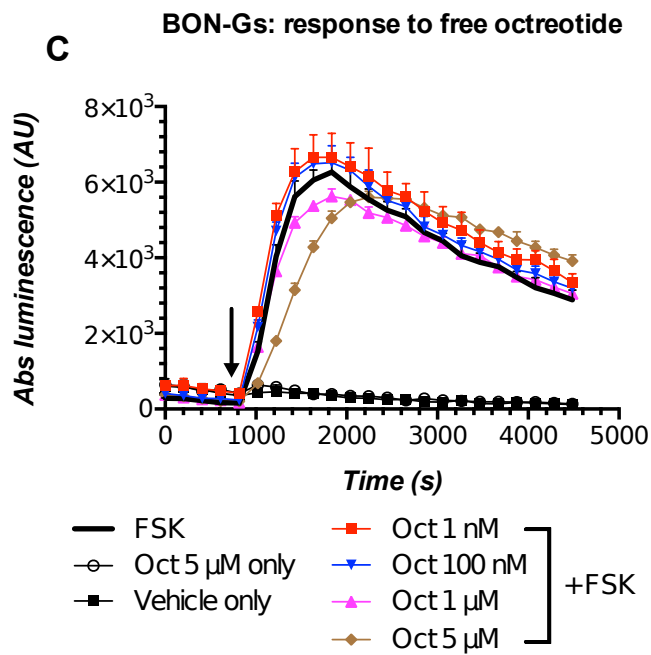
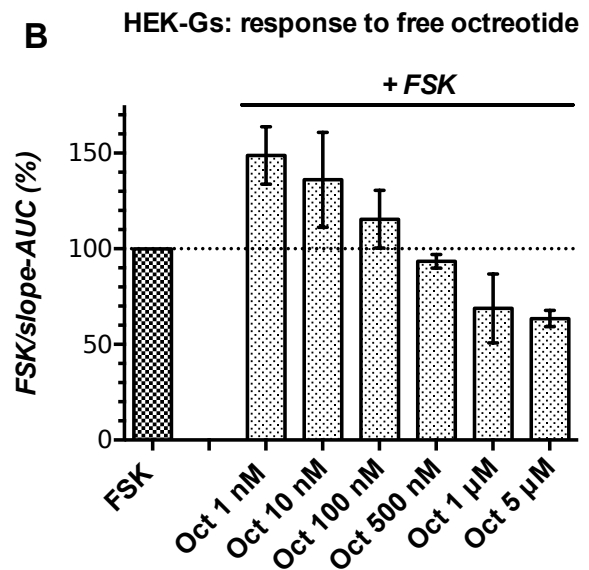
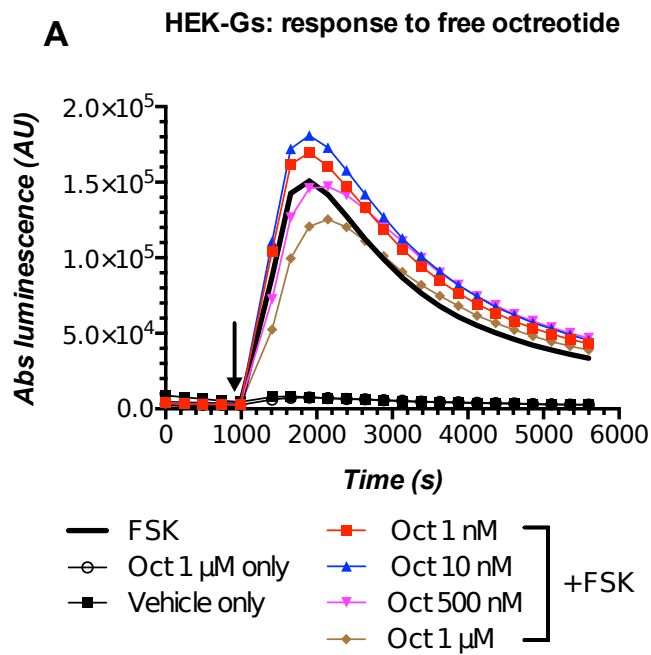
Supplementary Figure 2. Octreotide dose-response analyses in BON-Gs and HEK-Gs cells.

The assays were run at standard conditions (at RT, 200 μ M of IMBX and 10 μ M of FSK). Octreotide was added simultaneously with FSK; the moment of spiking is indicated with black arrow.

(A/C) Luminescence curves from a single representative runs (performed in triplicates) with varying concentrations of free octreotide in HEK-Gs and BON-Gs cells respectively. y-axis represents absolute luminescence values (AU); x-axis denotes time scale (s). Error bars on **panel C** represent mean \pm SD (with only SD's upper half shown); error bars on **panel A** are omitted for visual clarity.

(B/D) Collective results from the three independent runs with octreotide in HEK-Gs and BON-Gs respectively (in triplicates each), integrated by means of FSK/slope – AUC values (mean \pm SEM), as described in Materials and Methods section.

Evidently, only high – nanomolar (from 500 nM onwards) concentrations of octreotide were able to consistently lower cAMP levels in the cells under study. The nature of the *excitatory* effect of low-nanomolar concentrations of octreotide on FSK-induced cAMP generation in HEK-Gs and BON-Gs remains obscure and might warrant further investigation; however, in view of the pronounced inter-run variation and the moderate overall amplitude of cAMP changes, it has no practical relevance from the standpoint of testing of SSTR-targeted NPs.



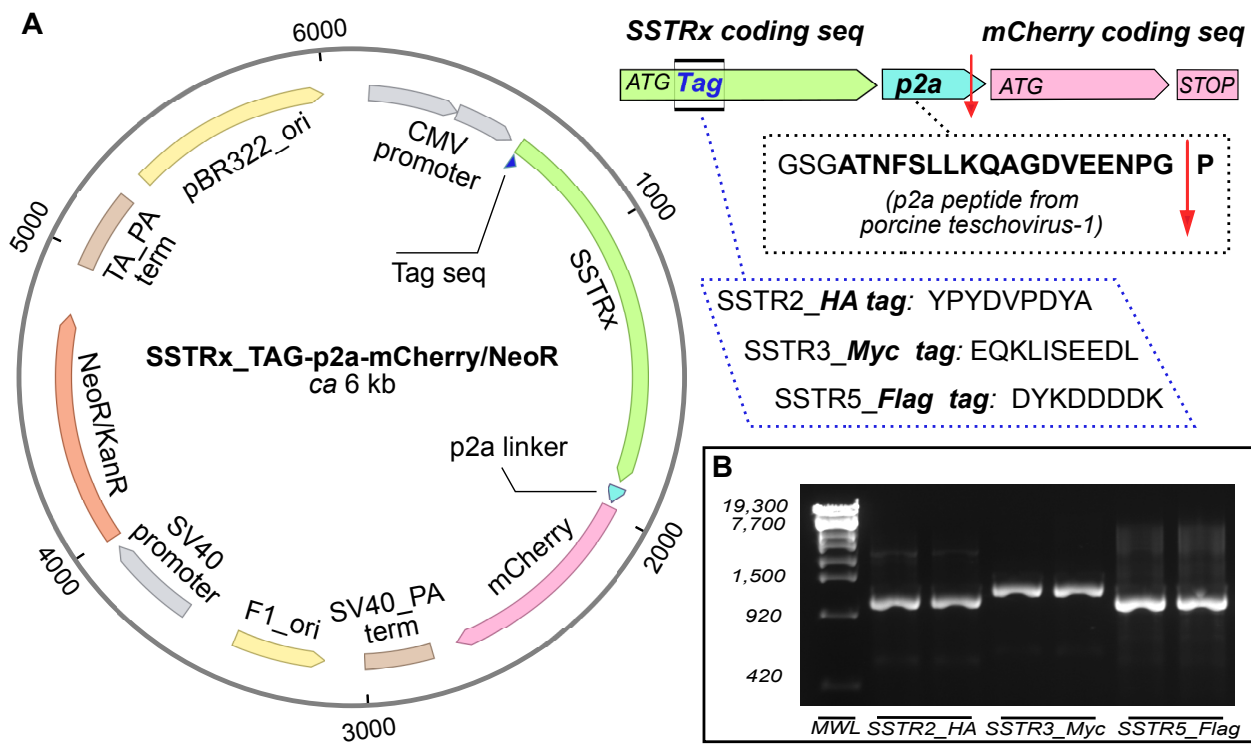
Supplementary Figure 3. Design and generation of SSTRx-P2A-mCherry expression plasmids.

(A) General structure of SSTRx-P2A-mCherry expression vectors and P2A linker in action.

Coding sequences of *SSTR2*, *3* and *5* genes were tagged with *HA*, *Myc* and *Flag* epitopes, respectively, by means of PCR amplification employing forward primers introducing the sequences for the specified tags immediately downstream of the start codon (ATG) of *SSTR* genes (refer to Table S2 for primer sequences). Tagging of SSTRs in the region of *N*-terminus has been shown to be neutral in terms of receptor trafficking and ligand-binding ability [1–3]. Next, the tagged sequences of *SSTR2*, *3* and *5* were coupled to *mCherry* fluorescent protein via P2A linker from porcine teschovirus-1 [4], and the resulting constructs were put under CMV promoter. Ribosomal skipping between *Gly* and *Pro* within the conserved region of P2A linker (indicated with *red vertical arrow*) during translation results in *self-cleavage* of the nascent protein pair, liberating balanced amounts of SSTRx and mCherry.

(B) Agarose gel electrophoresis of PCR-tagged coding sequences of *SSTR2*, *3* and *5*.

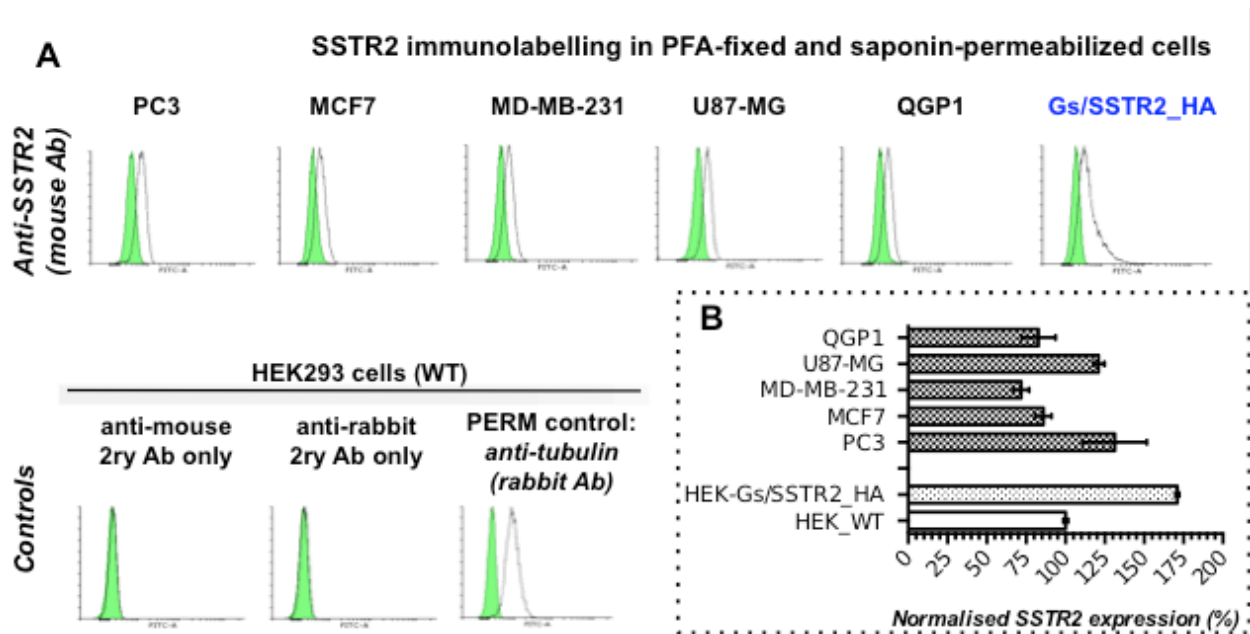
PCR products were resolved on 1.2% (w/v) agarose gel and stained with Ethidium Bromide (EtBr). The expected size of *SSTR2*_HA, *SSTR3*_Myc and *SSTR5*_Flag is 1147, 1297 and 1129 base pairs (bp) respectively. The target bands were cut out from the gel under LED light with a sterile scalpel, processed for DNA isolation and used in all the subsequent cloning steps, as described. *MWL* – molecular weight DNA ladder (lambda phage DNA digested with *StyI*; size of fragments - in bp).



Supplementary Figure 4. SSTR2 expression in HEK-Gs/SSTR2_HA vs selected non-modified cell lines.

(A) Overlay histograms of SSTR2 levels in the cell lines under comparison: black transparent charts stand for either non-stained controls or fully stained samples; shaded green charts reflect the corresponding secondary antibody – only stained controls. x-axis denotes sample emission [(505 nm longpass)/(530/30 nm bandpass)] upon stimulation with 488 nm laser; y-axis indicates the number of events registered. (B) As the cell lines in question have significantly different levels of autofluorescence, which translates to the differential positioning of SSTR2 histograms along x-axis and thus hinders efficient visual comparison, the actual SSTR2 signal is also demonstrated by means of bar charts, representing Geometric Mean (GeoMean) of the signal in the fully-stained cell populations subtracted with the average GeoMean of the corresponding non-stained controls, with the resulting values normalized to SSTR2 expression in HEK293 WT cells (100%); average values +/- SD are shown. As can be seen from **panels A** and **B**, some non-modified cell lines (PC3 and U87-MG) have comparable endogenous expression levels of SSTR2 to HEK-Gs/SSTR2_HA cells, whilst the target antigen abundance is lower in the others (QGP1, MD-MB-231 and MCF7). In principle, these results indicate physiological relevance of HEK-Gs/SSTR2_HA cells-based bioassay. Yet, as the net signalling outcomes in GPCR pathways are known to be dependent on relative abundance/availability of the downstream effectors and efficacy of their coupling (in case of cAMP transduction - G proteins, arrestins, G protein-coupled receptor kinases, ACs and PDEs; the list is not exhaustive), which can vary widely from cell line to cell line [5], similar receptor expression in any two given cell models would not immediately signify that these cells would have comparable response to the same dose of ligand in terms of receptor signalling. Thus, every cell model should be properly characterized for functional performance on a case-to-case basis.

Immunolabelling for SSTR2 with #MAB4224 mouse mAb was performed on PFA-fixed and saponin-permeabilized cells, as indicated in the Materials and Methods section; specificity of the mAb was earlier validated (Fig.2) Staining for β -tubulin, a component of a cytoskeleton, was implemented as a positive control of permeabilization. The cells were analyzed on LSRII cytometer; at least 20 000 of the gated events were captured. The data from a single representative experiment (performed in duplicate) is shown.



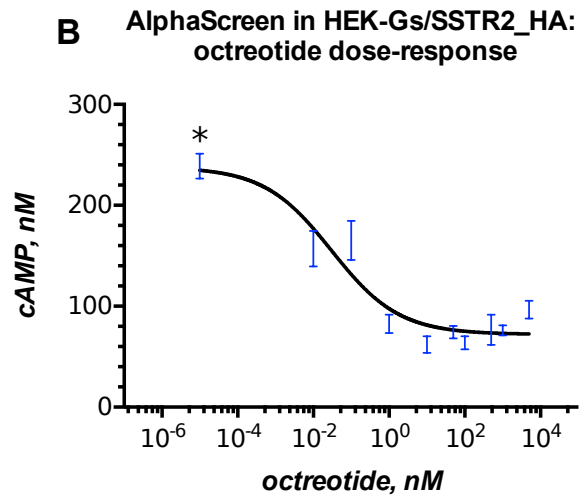
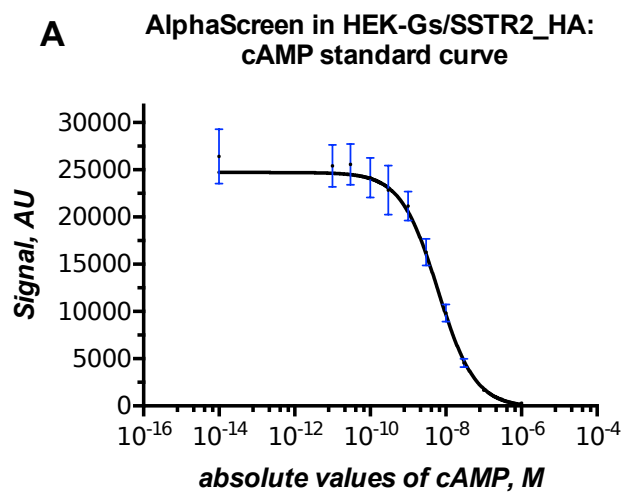
Supplementary Figure 5. Cross-validation of Gs22/cAMP assay with AlphaScreen cAMP test.

(A) cAMP standard curve. y-axis indicates AlphaScreen signal intensity (which is in essence a luminescence signal; AU); x-axis denotes cAMP concentration (M).

(B) Octreotide dose range in HEK-Gs/SSTR2_HA cells.

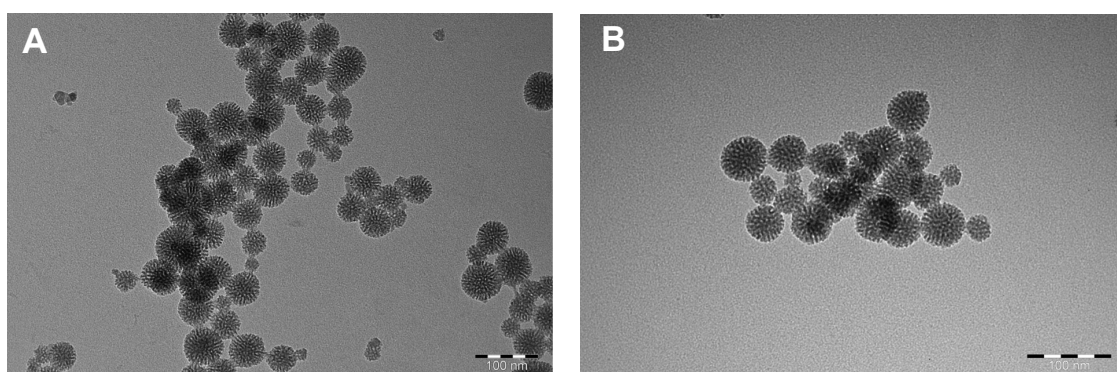
Absolute cAMP values were deduced from a standard curve (panel A) via «interpolate a standard curve» operator of GraphPad Prism software. Of note, all the effective octreotide concentrations fall well within the linear dynamic window of the assay (0.1 – 300 nM of cAMP; standard curve on **panel A**), indicating validity of the run. Maximum cAMP stimulation achieved with FSK only is indicated with an asterisk. y-axis demonstrates standard curve-derived absolute cAMP values (nM); x-axis denotes octreotide concentration (nM).

The assay was run in a 384-well plate format at RT with 10,000 HEK-Gs/SSTR2_HA cells per well in a final volume of 25 μ l. The cells were preincubated with 200 μ M IBMX and stimulated with FSK 10 μ M with or without octreotide. The reaction was stopped 10 min after stimulation, with subsequent lysis of the cells and signal capture on AlphaScreen technology-compatible platereader. Sigmoid dose-response curves were fitted with GraphPad Prism package. The results from a single representative experiment performed in three (3x) technical replicates (error bars are mean \pm SD) are shown; the assay was repeated three independent times overall.



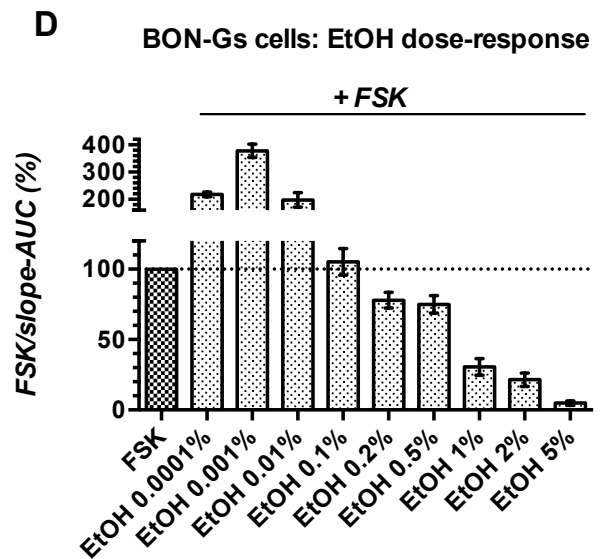
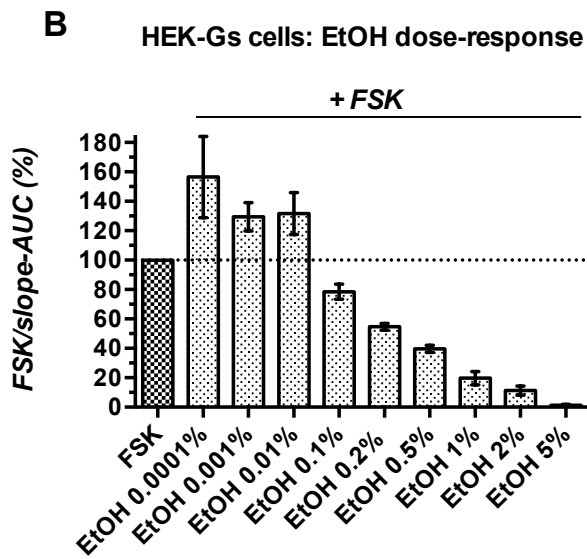
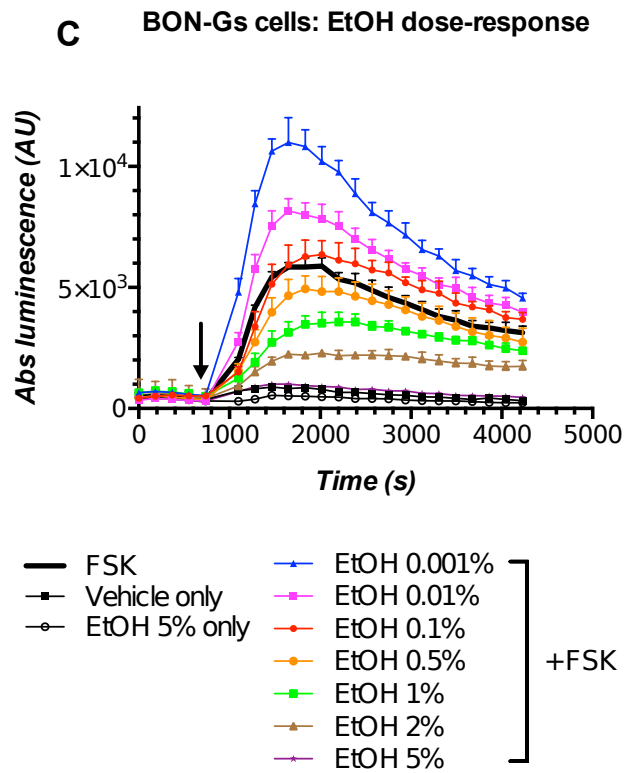
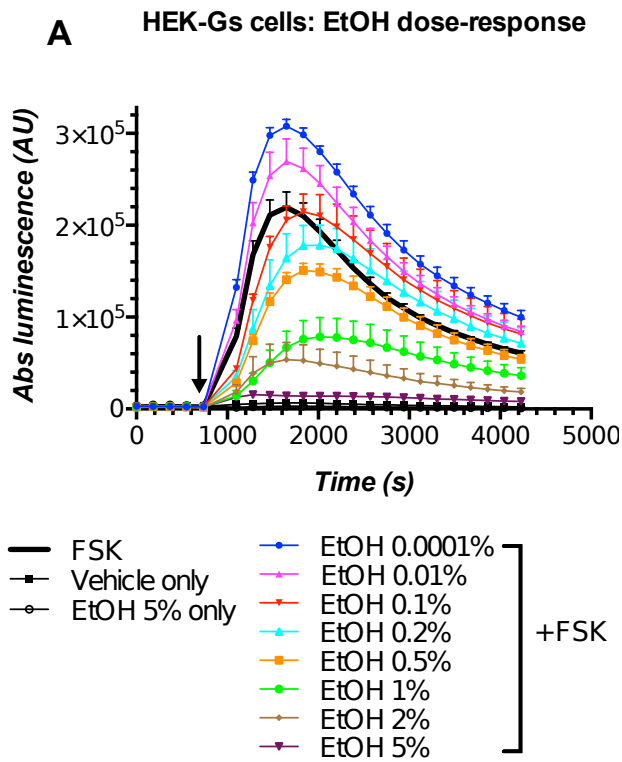
Supplementary Figure 6. MeSi-based nanocarriers maintain structural integrity over several months upon storage in A-EtOH.

TEM images of MeSi-based and PEI-functionalized NPs of average diameter 60-70 nm (in a dry state; MeSi₇₀-PEI), taken immediately after synthesis (**panel A**) and after *ca* 5 months of storage at +4°C suspended in A-EtOH (**panel B**).



Supplementary Figure 7. Dose-response studies of EtOH in Gs22/cAMP assay with HEK-Gs/SSTR2_HA and BON-Gs cells (**panels A-B** and **C-D** respectively). Evidently, EtOH affected light output in a non-linear fashion. The lowest concentrations tested [0.0001 – 0.01 % (v/v)] exerted a generally *excitatory* effect boosting light output up to 150% and 400% from FSK response in HEK-Gs/SSTR2_HA and BON_Gs cells, respectively. Still, higher levels of EtOH [from 0.1% (v/v) onwards] had inhibitory activity, producing dose-dependent signal depletion that culminated in a virtually complete abrogation of FSK response at 5% (v/v) of EtOH. Despite some differences in absolute level of the effect between the two cell types, i.e. low concentrations of EtOH stimulated light production in BON1 cells more potently than in HEK293 cells, which might be explained by differences in plasma membrane composition of these cells, the described general pattern of response to EtOH persisted, which might indicate the universal nature of the mechanisms involved.

The assays were run at standard conditions (at RT; 200 μ M of IMBX and FSK 10 μ M). The compounds were added to the cells simultaneously with FSK; the moment of spiking is indicated by the black arrow. **(A/C)** Luminescence curves observed in a single representative experiment performed in triplicates (mean values + upper half of SD are shown); x-axis denotes times scale (s), y-axis denotes non-normalized light output values (AU). **(B/D)** Results of three separate experiments combined, each performed in at least three technical replicates, with raw luminescence values converted to FSK/slope-AUC (%) index, as described in Materials and Methods. Error bars represent means +/- SEM.

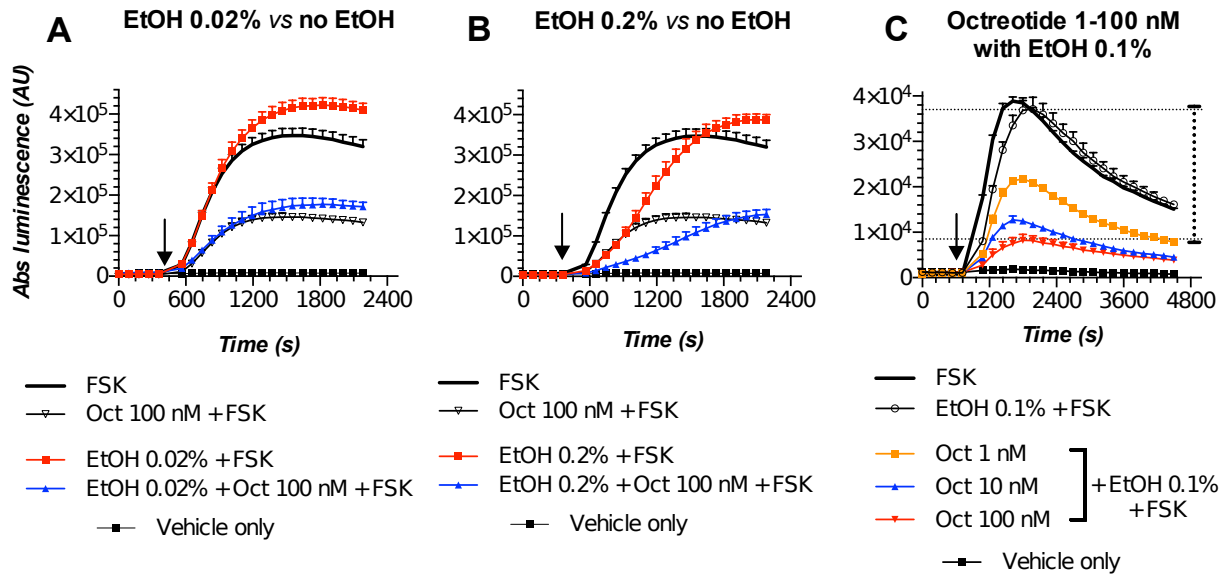


Supplementary Figure 8. EtOH modulates FSK-stimulated luminescence, but does not interfere with octreotide signaling in Gs22/cAMP assay.

EtOH effects on FSK-stimulated luminescence remain *imprinted* in the signal kinetics from the cells exposed to octreotide together with the matched concentration of EtOH. Suchwise, in cases of stimulatory activity of EtOH on FSK-induced luminescence, though co-treatment with octreotide results in net signal decline, both the peak signal and AUC in the octreotide/EtOH-treated cells remain higher than in the cells received the same concentration of octreotide without EtOH (**panel A**). The same holds true for higher levels of EtOH: whether exposure to EtOH «slows down» build-up of FSK-induced luminescence or lowers its amplitude, the described effects persist upon addition of octreotide (**panels B-C** and **C** respectively). Moreover, EtOH does not alter dose dependency of octreotide response (**panel C**). This data collectively demonstrates that EtOH acts as a modifier of FSK response and does not interfere with octreotide-evoked signaling.

Panel C also depicts the idea of resolving window of the assay in the presence of EtOH. Though EtOH at 0.1% (v/v) modifies kinetics of light output in response to FSK, the absolute amplitude of the signal stays high. This provides for a wide resolving window of inhibitory effects of octreotide, which in the present case can be approximated as the distance along y-axis (*depicted as a vertical line of black dots*) from the peak signal from the cells received EtOH 0.1% (v/v) with FSK to the peak signal from the cells exposed to 100 nM of octreotide (a concentration known to produce submaximal cAMP inhibition in SSTR2-overexpressing cells) together with the matched levels of FSK and EtOH. The assays were run with HEK-Gs/SSTR2_HA cells at standard conditions. The compounds were added to the cells simultaneously with FSK; the moment of spiking is indicated by the black arrow. **Panels A-C** demonstrate luminescence curves from single representative

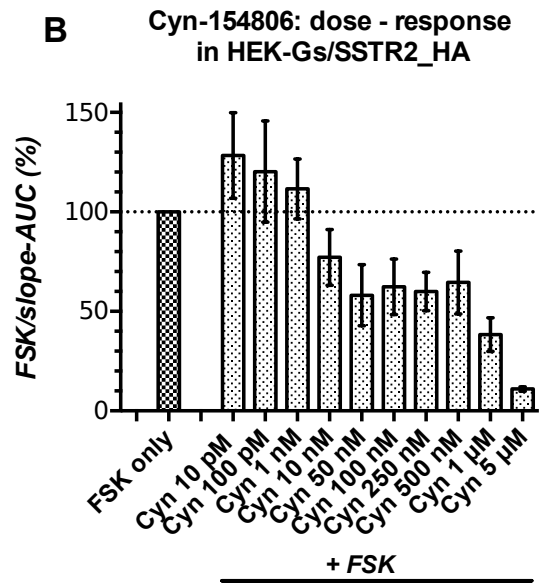
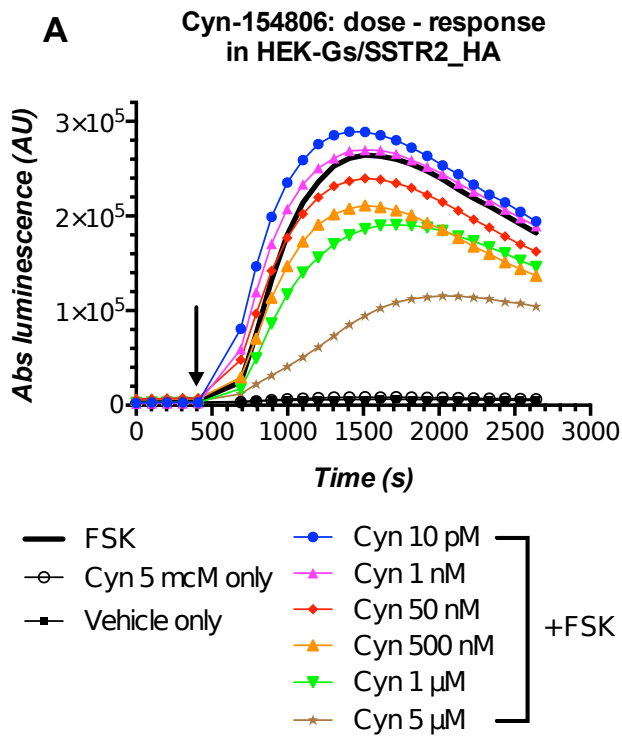
experiments performed in triplicates (mean values + upper half of SD are shown); x-axis denotes times scale (s), y-axis denotes non-normalized light output (AU).



Supplementary Figure 9. Cyn-154806 exerts dose-dependent effects on cAMP in SSTR2-overexpressing cells.

(A) Cyn-154806 dose-response in HEK-Gs/SSTR2_HA cells. Luminescence signal captured in a single representative run carried out in 3x technical replicates (mean values shown; SDs omitted for visual clarity) is shown; x-axis denotes times scale (s), y-axis denotes non-normalized light output (AU). (B) Cyn-154806 dose-response data from 3 independent experiments combined, with «raw» luminescence signal integrated by virtue of FSK/slope-AUC values (mean values +/- SEM), as described.

While low concentrations (10 pM – 1 nM) appeared to have a mild stimulatory effect on FSK-induced luminescence, higher levels of Cyn-154806 inhibited cAMP generation in HEK-Gs/SSTR2 cells in a dose-dependent manner. The inhibition became evident at a peptide concentration of 10-50 nM and continued to mount all the way to the highest concentration tested, 5 µM. Unlike octreotide, producing submaximal cAMP inhibition already at 10 nM (Figure 3A,C), Cyn-154806 exerted a potent inhibition of cAMP generation at levels of 500 nM and higher, with the magnitude of effect still lagging behind the one of octreotide at low-nanomolar concentrations. Together with the affinity profile (Table S1), this data highlights Cyn-154806 as a relatively weak (partial) agonist of SSTR2. The assays were performed at standard conditions. Cyn-154806 was added to the cells simultaneously with FSK; the moment of spiking is indicated by the black arrow.

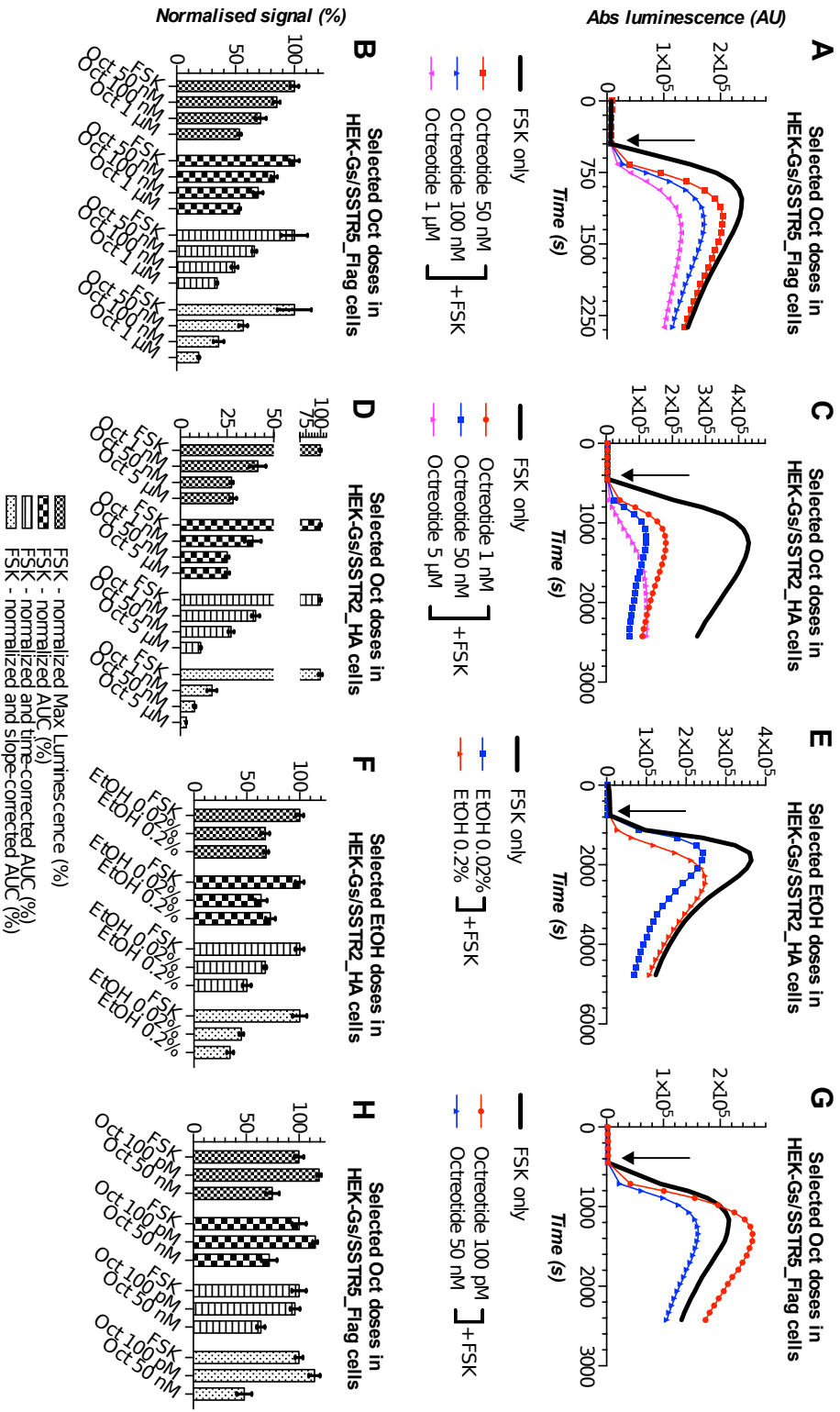


Supplementary Figure 10. Different types of luminescence curves in Gs22/cAMP assay and selection of a data processing approach.

Treatment with selected concentration of free octreotide in HEK-Gs/SSTR5_Flag and HEK-Gs/SSTR2_HA (**panels A-B/G-H** and **C-D** respectively). Effects of EtOH on FSK-induced light output in HEK-Gs/SSTR2_HA (**panels E-F**).

Panels A/C/E/G demonstrate luminescence curves; y-axis depicts absolute luminescence values (AU); x-axis denotes time scale (s). **Panels B/D/F/H** depict comparison of different approaches for raw data processing and normalization of the corresponding luminescence curves (**panels A/C/E/G** respectively); further explanations in the text.

The assays were run at RT as described in Materials and Methods, with the Induction Mix including 200 μ M of IMBX and a final concentrations of FSK 10 μ M. The compounds were added to the cells simultaneously with FSK; the moment of spiking is indicated by the black arrow. All the samples were processed in three (3x) technical replicates; error bars represent mean \pm SD (in **panels A/C/E/G** error bars omitted for visual clarity).



Supplementary information 1. Effects of EtOH on FSK-induced luminescence in Gs22/cAMP assay.

In Gs22/cAMP assay, EtOH acted as a non-linear modifier of FSK response: at concentrations as low as 0.0001 – 0.01% (v/v) EtOH had a marked *excitatory* activity, strongly potentiating FSK-induced light output in living cells, whilst higher concentrations of EtOH, from ca 0.05 – 0.1% (v/v) onwards, exerted clear dose-dependent inhibition of FSK-induced luminescence (Figure S7). Of note, this pattern of EtOH action was independently registered in two different human cell lines harboring Gs22/cAMP sensor, HEK293 and BON1, which were otherwise unrelated. Even more importantly, EtOH did not interfere with the inherent effects of targeting ligands and NPs on luminescence in Gs22/cAMP assay. Rather, the effects of EtOH, whether stimulatory or inhibitory, were reflected in the resulting kinetics of the signal from the cells exposed to either free targeting moieties or NPs together with matching concentrations of alcohol (Figure S8A-C).

The described effects of EtOH as a modifier of FSK response are likely to be of complex nature. There have been several reports on dose-dependent inhibition of FSK-induced cAMP generation by EtOH both in intact cells and membranous preparations, but the molecular machinery involved remains ill-defined: alterations in plasma membrane fluidity due to intercalation of alcohol molecules, leading to re-distribution of intramembranous lateral pressure, affecting tertiary conformation and activity of membrane-dwelling proteins (ACs), as well as direct effect of EtOH on catalytic subunits of ACs and/or their affinity to FSK have been speculated [6–12].

Supplementary information 2. Plasmid vectors for human SSTR2, 3 and 5.

> **SSTR5_Flag-P2A-mCherry plasmid** (5925 bp; accession #L T962381 at European Nucleotide Archive)

xxxxxx – Flag-tag

XXXX – SSTR5 coding sequence

XXXXXX – P2A sequence

XXXXXX – *mCherry* coding sequence

XXXXXX – *NEO* coding sequence

```
TAGTTATTAAAGTAATCAATTACGGGGTCAATTAGTTCATAGCCCATATAGGAGTTCGGGTTACATAACTTACGGTA
AATGGCCCGCCTGGCTGACCGCCCAACGACCCCGCCATTGACGTCAATAATGACGTATGTTCCCATAGTAACGCC
AATAGGCACTTTCATTGACCGTCAATGGGTGGAGTATTACGGTAACCTGCCACATTGGCAGTACATCAAGTGTATCA
TATGCCAAGTACGCCCCCTATTGACGTCAAITGACGGTAAATGGCCCGCCTGGCATTATGCCCAGTACATGACCTTAT
GGGACTTTCCTACTTGGCAGTACATCTACGTATTAGTCAATGCTATTACCATGGTGATGGGTTTTGGCAGTACATCA
ATGGGCGGTGATAGCGGTTTGACTCACGGGGATTTCCAAGTCTCCACCCCATTTGACGTC AATGGAGTTGTTTTGG
CACCAAAATCAACGGGACTTTC AAAAAITGCGTAACAACCTCCGCCCATTTGACGCAAAATGGCGGTAGGCCGTACG
GTGGGAGGTCTATATAAGCAGAGCTGGTTAGTGAACCGTCAGATCCCGTCTCCGTACGATGgattacaagatgatgatga
agGAGCCCCCTGTTCCAGCCTCCACGCGCCAGCTGGAACGGCTCC TCCCCGGGGGCTGCCCTCGGAGGCCGGTGACAA
CAGGACGCTGGTGGGCGCGCCCTCGGCAGGGGGCCCGGGGGTCTGCTGGTCCCGTCTGTACCTGCTGCTGTT
```

GTGCGGCCGGGCTGGCGGGAAACACCGCTGGTCATCTACGTGGTGGTGGCTTCGCCAAGATGAAGACCGTCACCA
ACATCTACATTCTCAACCTGGCAGTGGCCGACGTCCTGTACATGCTGGGGCTGCCTTTCC TGCCACCGAGAACGCC
GGCTCCTTCTGGCCCTTGGCCCGCTCCTGTGCCGCTGGTCATGACGCTGGACGGCGTCAACCAGTTCACCAGTG
TCTTCTGCCTGACAGTCATGAGCGTGGACCCTACCTGGCAGTGGTGCACCCGCTGAGCTCGGCCCGCTGGCGCC
GCCCGCGTGTGCCAAGCTGGCGAGCCCGCGGCTGGGTCTGTCTGTGCATGTGCTGCCGCTCCTGGTGT
TCGCGGACGTGCAGGAGGCGGTACCTGCAACGCCAGCTGGCCGGAGCCCGTGGGGCTGTGGGCGCCGCTTTC
ATCATCTACACGGCCGTGCTGGCTTCTTCCGCCGCTGCTGTATCTGCCCTGTGCTACCTGCTCATCGTGGTGAA
GGTGAGGGCGCGGCGTGCCTGGCTGCCGTGCCGGCGGCTCGGAGCGGAAGGTGACCGCGCATGGTGTG
GTGGTGTGCTGGTGTGGCGGATGTGGCTGCCCTTCTTACCCTCAACATGTC AACCTGGCCGTGCCGTGC
CCAGGAGCCCGCTCCGCCGCTACTTCTTGTGTATCTCTACGCCAACAGCTGTGCCAACCCCGT
CCTCTACGGCTTCTCTCTGACAACCTCCGCCAGAGCTTCCAGAAAGTTCTGTGCCCTCCGCAAGGGCTCTGGTGCCA
AGGACGCTGACGCCACGGAGCTGCCGTCAGACAGGATCCGGCAGCAGGAGGCCACCGCCGCCACCCG
GCCGACGCCAACGGCTTATGCAGACCAGCAAGCTGGCCGCAGACGGAAAGCGGAGCTACTAAGCTTCTGAGCCTG
CTGAAGCAGGCTGGCGACGTGAGGAGAAACCTGGAACCTGATGGTGAAGCAAGGGCGGAGGAGGA
TAACATGGCCATCATCAAGGAGTTCATGCCCTTCAAGGTGCACATGGAGGGCTCCGTGAACGGCCACAGATTGAG
ATCGAGGGCGAGGGCGGCCCTACGAGGGCACCCAGACCCCAAGCTGAAAGGTGACCCAAGGGTGGCCC
CCTGCCCTTGCCCTGGACATCCTGTCCCTCAGTTGATGTACGGCTCCAAGGCTACGTGAAAGCACCCCGCCGAC
ATCCCGGACTACTTGAAGCTGTCCCTCCCGGAGGGCTTCAAGTGGGAGCGCGTGATGAACCTCGAAGGACGGCGCG
TGGTGACCGGTGACCCAGGACTCCTCCCTGCAAGGACGGCGAGTTTACATCTACAAAGGTGAAGCTGCCCGGCAACCACTT

CCCCCTCCGACGGCCCCGTAATGCAGAAGAAGACCATGGGCTGGGAGGCCCTCCTCCGAGCGGATGTACCCCGAGGACGGCCCTGAAGGGCGAGATCAAGCAGAGAGGCTGAAGCTGAAGGACCGGCCACTACGACCGCTGAGGTCAAGAC
CACCTACAAGGCCAAGAAGCCCGTGCAGCTGCCCGGGCCCTACAACGTCAACATCAAGTTGGACATCACCTCCAC
AAGGAGACTACACCATCGTGGAAACAGTACGAACGGCCGAGGGCCGCCACTCCACCCTCCGGCATGGACGAGCTG
TACAAGTCCGGAAACTAGTCTCAGATCTGAGCTCAAGCTTCGAATTCGCAGTCGACGGTACCGGGCCCGGGA
TCCACCGGATCTAGATACTGATCATAATCAGCCATACCACATTTGTAGAGGTTTACTTGCTTAAAAAACCTCCAC
ACCTCCCCCTGAACCTGAACACATAAAAAATGAATGCAATTTGTTGTTAACTTGTATTGCAGCTTATAATGTTACAAA
TAAAGCAAATAGCATCACAAAATTCACAAAATAAAGCATTTTTTTCACCTGCATTTAGTTGTGTTGCCAAACTCATCAA
TGATCTTAACGCGTAAATTTAAGCGTTAATATTTTGTAAAAATTCGCGTTAAATTTTTGTTAAATCAGCTCATTTTTTA
ACCAATAGGCCGAAAATCGGCAAAATCCCTATAAATCAAAAAGATAGACCGAGATAGGTTGAGTGTTGCCAGTTT
GGAACAAGAGTCCACTATTAAGAACGTTGGACTCCAACGTCAAAAAGGGCGAAAAAACCGTCTATCAGGGCGATGGCCCA
CTACGTGAACCATCACCCTAATCAAGTTTTTTGGGTCGAGGTGCCGTAAAGCACTAAATCGGAACCCTAAMGGGAG
CCCCCGATTTAGAGCTTGACGGGGAAAGCCGGGAACGTGGCGAGAAAAGGAAGGAAAGCGAAAAGGAGCGGG
CGCTAGGGCGCTGGCAAGTGTAGCGGTCACGCTGCCGTAACCAACACCCCGCCTAATGCCCGCTACA
GGGCGCGTCAGGTGGCACTTTTCCGGGAAATGTGCCGGGAACCCCTATTTGTTATTTTTCTAAAAATACATTTCAAAATAT
GTATCCGCTCATGAGACAAITAACCCTGATAAATGCTTCAATAATAATTGAAAAAGGAAAGAGTCTGAGGCGGAAAAAGAAC
CAGCTGTGGAATGTGTGTCAGTTAGGGTGTGAAAAGTCCCCAGGCTCCCCAGCAGGCAAGATATGCAAAAAGCATGC
ATCTCAATTAGTCAGCAACCAGGTGTGAAAAGTCCCCAGGCTCCCCAGCAGGCAAGAAATATGCAAAAAGCATGCATCTC
AATTAGTCAGCAACCATAGTCCCGCCCTAACTCCGCCCATCCCGCCCTAACCTCCGCCAGTTCGCCCATTTCTCC

GCCCCATGGCTGACTAATTTTTTTATTATGACAGAGGCCGAGGCCCTCGGCTCTGAGCTATTCAGAAGTAGT
GAGGAGCCTTTTTGGAGCCTAGGCTTTTGCAAGATCGATCAAGAGACAGAGTAGGATCGTTCCG**ATGATTGA**
ACAAGATGATTGCACGCAGGTTCTCCGGCCGCTTGGGTGAGAGGCTATTCGGCTATGACTGGCACACAACAGACA
ATGGCTGCTCTGATGCCGCCGTGTTCCGGCTGTACCCGACGGGGCCCGGTTCTTTGTCAAGACCAGACCTGT
CCGGTGCCCTGAATGAAC TGCAAGACGAGGCAGCCGGCTATCGTGGCTGGCCACGACGGCCGTTCCTTGCCAG
CTGTGCTGACGTTGTCACTGAAAGCCGGGAAGGACTGGCTGCTATTGGCGAAGTGCCGGGACAGGATCTCCTGTC
ATCTCACCTTGCTCCTGCCGAGAAAGTATCCATCATGGCTGATGCAATGCCGGCTGCATAACGCTTGATCCGGCTA
CCTGCCCATTCGACCACCAAGCGAAACATTCGCATCGAGCCGACGTA CTGGATGGAAGCCCGGCTTGTGCATCA
GGATGATCTGACGGAAGAGCATCAGGGCTCGCCGACCCGAAC TGTTCGCCAGGCTCAAGGCCGAGCATGCCCGA
CGGCGAGGATCTCGTCTGACCCATGGCGATGCC TGTGCCGAATATCATGGTGGA AAATGGCCGCTTTCCTGGAT
TCATCGACTGTGGCCGGCTGGGTGTGGCCGACCGCTATCAGGACATAGCGTTGGCTACC CGTGATATTGCTGAAGA
GCTTGGCCGGCAATGGGCTGACCCGCTTCCTCGTGC TTTACGGTATGCCCGCTCCCGATTCCGACGGCATCGCCTTC
TATCGCC TTTGACGAGTTCTTCTGA GCGGGACTCTGGGTTCGAATGACCGACCAAGCGACGCCCAACCTGCCA
TCACGAGATTTGATTCACCCGCCCTTCTATGAAAGGTTGGGCTTCGGAATCGTTTTCCGGGACGCCGGCTGGAT
GATCCTCAGCGGGGATCTCATGCTGGAGTTC TCCGCCACCCTAGGGGAGGCTAACTGAAACACGGAAAGGAG
ACAATACC GGAAAGAACCCCGCTATGACGGCAATAAAAGACAGAAATAAAACGCACCGTGTGGGTGTTGTTCA
TAAACGCGGGGTTGGTCCAGGGCTGGCACTCTGCATACCCACCGAGACCCATTGGGGCCAATACGCCCGC
GTTTCTCCTTTCCCCACCCACC CCAAGTTCGGGTGAAGGCCAGGGCTCGCAGCCAAACGTCGGGGCCGACAG
GCCCTGCCATAGCCTCAGGTTACTCATATACTTTAGATTGATTTAAAACTTCATTTTAATTTAAAAAGGATCTAGGTG

AAGATCCTTTTGTGATAATCTCATGACCAAAATCCCTTAACGTGAGTTTTCGTTCCACTGAGCGTCAGACCCCGTAGAAA
AGATCAAAGGATCTTCTTGAGATCCTTTTTTCTGGCGTAATCTGCTGTTGCAAAACAAAAAACCCACCGCTACCAG
CGGTGGTTTGTGGCCGATCAAGAGCTACCACACTTTTTCCGAAGGTAAC TGGCTTCAAGCAGAGCGCAGATACCA
AATACTGTCCTTCTAGTGTAGCCGTAAGTTAGGCCACCACCTTCAAGAACTCTGTAGCACCGCCTACATACCCTCGCTCTG
CTAATCCTGTTACCAGTGGCTGCTGCCAGTGGCGAITAAGTGTGTCTTACC GG GTTGACTCAAGACGATAGTTACC
GGATAAGCGCGCAGCGGTCGGGCTGAACGGGGGTTCGTGCACACAGCCAGCTTGAGCGAAACGACCTACACCCGA
ACTGAGATACCTACAGCGTGAAGCTATGAGAAAAGCCACGCTTCCCGAAGGGAAGAAAGCGGACAGGTATCCGGTA
AGCGGCAAGGTCGGAACAGGAGAGCGCACGAGGGAGCTTCCAGGGGGAAACGCCCTGGTATCTTATAGTCCTGTC
GGGTTTCGCCACCTCTGACTTGAGCGTCGATTTTTGTGATGCTCGTCAGGGGGGAGCCTATGAAAAAACGCCA
GCAACGGCGCCTTTTACGGTTCCTGGCCTTTTGCTGGCCTTTGCTCACATGTTCTTCTGCGTTATCCCTGATT
CTGTGGATAACCGTATTACCGCCATGCAT

>**SSTR2_HA - P2A-mCherry plasmid** (5932 bp; accession #L_T962382 at European Nucleotide Archive)

xxxxxxx – HA-tag

XXXXX – SSTR2 coding sequence

XXXXXX – P2A sequence

XXXXXX – mCherry coding sequence

XXXXXX – NEO coding sequence

TAGTTATTAAAGTAATCAATTACGGGGTCAATTAGTTCAITAGCCCATATATGGAGTTCGGGTTACATAACTTACGGTA
AATGGCCCCCTGGCTGACCGCCCAACGACCCCGCCATTGACGTCAAITAATGACGATATGTTCCCATAGTAACGCC
AATAAGGACTTTCATTGACGTCATGGGTGGAGTATTAACGGTAAACTGCCACTTGGCAGTACATCAAGTGTATCA
TATGCCAAGTACGCCCCCTATTGACGTCATGACGGTAAAATGGCCCGCCTGGCATTATGCCCAGTACATGACCTTAT
GGGACTTTCCTACTTGGCAGTACATCTACGTATTAGTCATCGCTATTACCATGGTGATGCCGTTTGGCAGTACATCA
ATGGGCGTGGATAGCGGTTTGACTCACGGGATTCCAAAGTCTCCACCCCATTGACGTC AATGGGAGTTGTTTGG
CACCAAAATCAACGGGACTTTC AAAATGTCGTAACAACCTCCGCCCATTTGACGCAAAATGGCGGTAAGCGGTACG
GTGGGAGGTCTATAITAAGCAGAGCTGTTTAGTGAACCGTCAGATCCCGTCTCCCGTACGATG**accatac**
acgcGACATGGCGATGAGCCACTCAATGGAAGCCACACATGGCTATCCATTCCAITTGAACCTCAATGGCTCTGTGGT
GTCAACCAACACCCTCAAAACCAGACAGAGCCGTACTATGACCTGACAAGCAATGCAGTCCCTCACATTCATCTATTTGT
GGTCTGCATCATTGGGTTGTGTGGCAACACACTTGTCAITTTATGTCACTCTCCGCTATGCCAAGATGAAGACCATCAC
CAACATTTACATCCTCAACCCTGGCCATCGCAGATGAGCTCTTCATGCTGGGCTGCCCTTCTTGGCTATGCAGGTGGC
TCTGGTCCACTGGCCCTTGGCAAGGCCATTTGCCGGGTGGTCACTGTGATGGCATCAATCAGTTTACCACAGCA
TCTTCTGCCCTGACAGTCATGAGCATCGACC GATACCTGGCTGTGGTCCACCCCATCAAGTCGGCCAAGTGGAGGAG
ACCCCGGACGGCCAAGATGATCACCATGGCTGTGGGAGTCTCTGCTGTGTCATCTTGCCCATCATGATATATG
CTGGGCTCCGGAGCAACCAGTGGGGAGAAAGCAGCTGCACCATCAACTGGCCAGGTGAATCTGGGGCTTGGTACA
CAGGGTTCATCATCTACACTTTCATTCTGGGTTCCGTGTAACCCCTCACCATCATCTGTCTTGGCTACCCTGTTCAATTAT
CATCAAGGTGAAGTCCCTCTGGAATCCGAGTGGGCTCCCTCTAAGAGGAAAGAGTCTGAGAAAGAAAGTCCACCCGAATG
GTGTCATCGTGGTGGCTGTCTTTCATCTTCTGCTGGCTGCCCTTCTACATAATTCACGTTTCTCCGCTCCATGGCC

ATCAGCCCCACCACCAGCCCTTAAAGGCATGTTTGACTTTGTGGTCCCTCACCATATGCTAACAGCTGTGCCAACCC
TAICCTAATATGCCTTCTTGTCTGACAACCTTCAAGAAGAGCTTCCAGAATGTCTCTGCTTGGTCAAGGTGAGCGGCAC
AGATGATGGGAGCGGAGTGACAGTAAAGCAGACAATCCCGGCTGAATGAGACCACGGAGACCAGAGACCCAGAGACCCCT
CCTCAATGGAGACCTCCAACCAGTATCGGAAGCGGAGCTACTAACTTGAGCCCTGCTGAAGCAGGCTGGCCGACGT
GGAGGAGAACCCTGGACCTGGTCTCCGGCCGATGGTGAGCAAGGGCGAGGAGGATAACATGGCCATCATCAAGGA
GTTCATGCGCTTCAAGGTGCACATGAGGGCTCCGTGAACGGCCACGAGTTCGAGATCGAGGGCGAGGGCGGAGGG
CCGCCCTACGAGGGGCACCAGCCGCCAAGCTGAAGGTGACCAAAGGTGGCCCTGCCCTGGCCTGGGACAT
CCTGTCCCCTCAGTTTATGTACGGCTCCAAGGCCCTACGTGAAGCACCCCGCGACATCCCCGACTTGAAGCTGT
CCTTCCCCGAGGCTTCAAGTGGAGCGCGTGATGAACCTTGAGGACGGCGGCGTGGTGACCCTGACCCAGGACT
CCTCCCTGCAGGACGGCGAGTTTATCTACAAGGTGAAGCTGCGCGGCACCAACTTCCCCTCCGACGGCCCCGTAAT
GCAGAAAGAAGACCATGGGCTGGGAGGCCCTCCTCCGAGCGGATGTACCCCGAGACGGCCCTGAAAGGGCGAGAT
CAAGCAGAGGCTGAAGCTGAAGGACGGCCGACTACGACGCTGAGGTCAAAGACCACCTACAAGGCCAAGAACCC
CGTGCAGCTGCCCGGCGCCTACAACGTCAAACATCAAGTTGGACATCACCTCCACACAAGAGGACTACACCATCGTG
GAACAGTAGGAACGGCCGAGGGCCGACCTCCACCGGGGCATGGACGAGCTGTACAAGTCCGGAAACTAGTCT
CAGATCTCGAGCTCAAGCTTCGAATTCTGCAGTCGACGGTACCGGGGCCGGGATCCACCGGATCTAGATAACTG
ATCATAATCAGCCATACCACATTTGTAGAGGTTTACTTGTCTTAAAAAACCTCCACACACCTCCCCCTGAACCTGAAAC
ATAAAATGAATGCAATTTGTTGTTAAGTTTATTGCAAGCTTATAATGTTACAATAAAGCAATAGCATCACAAAT
TTCACAAATAAAGCATTTTTTTCACCTGCATTTAGTTGTGGTTGTCCAAACTCATCAATGTATCTTAACGGCGTAAATTG
TAAGCGTTAATATTTTGTAAAAATTCGGGTTAAATTTTGTAAATCAGCTCATTTTTTAACCAATAGGCCGAAATCGGC

AAAATCCCTTATAAATCAAAAGAATAGACCGAGATAGGGTTGAGTGTTCAGTTTGAACAAGAGTCCACTATTAA
AGAACGTGGACTCCAACGTCAAAGGGCGAAAAACCCTCTATCAGGGCGATGGCCACTACGTGAACCATCACCCTTAA
TCAAAGTTTTTGGGGTCGAGGTGCCGTAAGCACTAAATCGGAACCCCTAAAGGGAGCCCCCGATTAGAGCTTGACG
GGAAAAGCCGGCGAACGTGGCGAGAAAAGGAAGGAAAGCGAAAAGGAGCGGGCGCTAGGGCCGTGGCAAGTG
TAGCGGTCACCGCTGCCGGTAACCACCACCCCGCCGCTTAATGCCCGCTACAGGGCGCGTCAGGTTGGCACTTT
TCGGGAAATGTGCCGGAAACCCCTATTGTTATTTTCTAAATACATTCAATATGTATCCGCTCATGAGACAATAA
CCCTGATAAATGCTTCAATAATAATTGAAAAAGGAAGAGTCCGTAGGGCGGAAAAGAACCAAGCTGTGGAATGTGTGTCAGT
TAGGGTGTGAAAAGTCCCACAGGCTCCCACGAGGCGAGAAGTATGCAAAAGCATGCATCTCAATTAGTCAGCAACCAG
GTGTGAAAGTCCCAGGCTCCCAGAGGCGAGAAGTATGCAAAAGCATGCATCTCAATTAGTCAGCAACCATAGTCC
CGCCCTAACTCCGCCATCCCGCCCTAACTCCGCCAGTTCGCCCATTTCTCGCCCATGGCTGACTAATTTTT
TTTATTTATGCAGAGGCCGAGGCCCTCGGCCCTGAGCTAATCCAGAAGTAGTGAGGAGGCTTTTTGGAGGCCCT
AGGCTTTTGCAAAGATCGATCAAGAGACAGGATGAGGATCGTTTCGCATGATTGAACAAGATGGATTGCACCGCAGGT
TCTCCGGCCGCTTGGGTGAGAGGCTATTGGCTATGACTGGGCACACAGACAATCGGCTGCTCTGATGCCGCCG
TGTTCCGGCTGTGAGCGCAGGGGCCCGGTTCTTTTGTCAAGACCAGCCTGTCCGGTGCCTGAATGAACCTGCA
AGACGAGGCGAGCGCGCTATCGTGGCTGGCCACGACGGCGTTCCTTGCCGAGCTGTGCTGACGTTGTCACTGA
AGCGGGAAGGACTGGCTGCTATTGGCGAAGTGCCGGGGCAGGATCTCCTGTCAATCTCACCTTGCTCCTGCCGAG
AAAGTATCCATCATGGCTGATGCAATGCGGGCTGCATACGCTTGATCCGGCTACCTGCCAATTCGACCACCAAGC
GAAACATCGCATCGAGCGAGCACGCTACTGGATGGAAGCCGGTCTTGTGATCAGGATGATCTGGACGGAAGAGCAT
CAGGGGCTCGCCACAGCCGAACCTGTTGCCACAGGCTCAAGGCGAGCATGCCCGACGGCGAGGATCTCGTCTGACC

CATGGCGATGCCCTGCTTGCCGGAATATCATGGTGGAAAAATGGCCGCTTTCTGGATTTCATGCACTGTGGCCGGCTGGC
TGTGGCGGACCCTATCAGGACATAGCCGTTGGCTACCCTGTATATTGCTGAAGAGCTTGGCCGCAATGGCCTGAC
CGCTTCCCTGCTGCTTACGGTATGCCCGCTCCCGATTGCGAGCGCATCGCCTTCTATGCCCTTTGACGAGTTCTTC
TGA

GGGACTCTGGGTTGAAATGACC

GACC

CAAGCGCCCAACCTGCCATCAGGATTTGATTCACCCG
CGCCTTCTATGA

AGGTTGGGCTTCGGAATCGTTTTCCGGGACGCCGGCTGGATGATCCTCAGCCGGGGATCTC
ATGCTGGAGTTC

CGCCACCCCTAGGGGAGGCTAACTGA

AACCGGAAGGAGACATACCGGAAGCAACCCCGC
CTATGACGGCAATAAAAAAGACAGAATAAAACGCACGGTGTGGGTCGTTTTCATAAACGGGGTTCGGTCCAG
GGCTGGCACTCTGTGATACCCCA

CGAGACCCCATTTGGGCCAATA

CGCCCGGCTTCTCCACCCCA
CCCCCAAGTTGGGTGAAGGCCCAGGGCTCGCAGCCAACGTCGGGGCGGCAAGCCCTGCCATAGCCTCAGGTTA
CTCATA

TACTTTAGATTGATTTAAAC

TTTCATTTTAA

TTTAAAGATCTAGGTGAAGATCCTTTTGATAATCTCAT
GACCAAAA

TCCCTTAACGTGAGTTTTGTTCCACTGAGCGTCAGACCCCGTAGAAAAAGATCAAAAGGATCTTCTTGAGA
TCCTTTTTTTCTGCGCGTAATCTGCTGCTTGCAAAACAAAAAACCA

CCGCTACCAGCGGTGTTGCCC

GATCA

AGAGCTACCAACTCTTTTCCGAAGGTA

ACTGGCTT

CAGCAGACGCGAGATACCAAA

TACTGTCTTAGTGTAGCC
GTAGTTAGGCCACCACTTCAAGAACTCTGTAGCACCGCCTACATACTCGCTCTGCTAATCCTGTTACCAGTGGCTGC
TGCCAGTGGCGATAAGTGTGTCTTACC

GGTTGACTCAAGACGATAGTTACC

GGATAAGCGCGGTCGGGC
TGAACGGGGGTTGTCGCACACAGCCAGCTTGAGCGAACGACCTACACCGAACTGAGATACCTACAGCGTGAGC
TATGAGAAAAGCGCCACGCTTCCCGAAGGGAGAAAAGCGGACAGGTA

TCCGGTAAGCGGCAGGT

CGGAACAGAGAG
AGCGCACGAGGGAGCTTCCAGGGGAAAAACGCCCTGGTATCTTATAGTCC

TGTGCGGTTTCGCCACCTCTGACTTGA
GCCGTCGATTTTGTGATGCTGTCAGGGGGCGGAGCCCTATGGAAAAACGCCAGCAACGGCCCTTTTACCGGTT

CTGGCCTTTTGGCCTTTTGGCTCACATGTTCTTTCCTGCCGTTATCCCGTATTCTGTGGATAACCGTATTACCGCCA
TGCAI

> **SSTR3_Myc-P2A-mCherry plasmid** (6093 bp; accession #L T962383 at European Nucleotide Archive)

xxxxxx – Myc-tag

XXXX – SSTR3 coding sequence

XXXXXX – P2A sequence

XXXXXX – mCherry sequence

XXXXXX – NEO coding sequence

TAGTTATTAAITAGTAATCAATTACGGGGTCAATTAGTTCAATAGCCCATATATGGAGTTCGGGTTACATAACTTACGGTA
AATGGCCCGCCTGGCTGACC GCCCAACGACCCCGCCATTGACGTCAAITAAATGACGTATGTTCCCATAGTAACGCC
AATAGGACTTTCATTGACGTCATGGGTGAGTATTACGGTAAACTGCCACTTGGCAGTACATCAAGTGTATCA
TATGCCAAGTACGCCCCCTATTGACGTCATGACGGTAAATGGCCCGCTGGCATTATGCCCAGTACATGACCTTAT
GGGACTTTCCTACTTGGCAGTACATCTACGTATTAGTCATCGCTATTACCATGGTGATGGGTTTTGGCAGTACATCA
ATGGGCGTGGATAGCGGTTTGACTCACGGGATTTCCAAGTCTCCACCCCATTTGACGCAAAATGGCGGTAGCGGTACG
CACCAAAATCAACGGGACTTTCCAAAAATGTCGTAACAACCTCCGCCCATTTGACGCAAAATGGCGGTAGCGGTACG
GTGGGAGGTCTATATAAAGCAGAGCTGGTTTAGTGAACCGTCAGATCCCGTCTCCGTACGATGgaacaaaaaaactcctcagaa
gagatctfgGACATGCTTCATCCATCATCGGTGTCACAGACCTCAGAACCCTGAGAAITGCCCTCGGCCCTGGCCCCCAG

ATGCCACCCTGGGCAACGTTGCGGGGGCCCAAGCCCGGCAGGGCTGGCCGTCA GTGGCTTCTGATCCCCCTGG
TCTACCTGGTGTGCGTGGTGGCCCTGCTGGTAACTCGCTGGTCA TATATGTGTCCTGGCACACGGCCAG
CCCTTCA GTCACCAACGTTACATCCTCAACCTGGCGCTGGCCGACGAGCTCTTCATGCTGGGGCTGCCCTTCCTGG
CCGCCAGAACGCCCTGTCTACTGGCCCTTGGCTCCCTCATGTGCCCGCTGGTCATGGCGGTGATGGCATCAA
CCAGTTCACCAGCA TATTCTGCC T GACTGTCA TGAGCGTG GACC GCTACCTGGCCG GTGTACATCCACC CGCTCG
GCCCGCTGGCGACAGCTCCGGTGGCCCGCAGCGT CAGCGCGCTGTGTGGTGCCCTCAGCCGTGGTGTGCT
GCCCGTGGTCTTCTCGGGAGT GCCCGCGGCATGAGCACCTGCCACATGCAGTGGCCGAGCCGGCGGGG
CCTGGCGAGCCGGCTTCATCATACACGGCCGCACTGGGCTTCTTGGGCCGTGCTGTGTCATCTGCCCTCTGCTA
CCTGCTCATGTGTGAAGGTGCGCTCAGCTGGCGCCGGGTGTGGCACCCCTCGTGCCAGCGGGCGGGCGCT
CCGAACGCAGGGTCA CGCGCATG GTGGTGGCCGTGGTGGCGCTCTTGTCTGCTGCTGATGCCCTTCTACGTGCT
CAACATCGTCAACGTGGTGTGCCCACTGCCCGAGGAGCCTGCC TTTGGGCTTACTTCC TGGTGGCGCTG
CCCTATGCCAACAGCTGTGCCAACCCCA TCTTATGGCTTCTCTCC TACC GCTTCAAGCAGGGCTTCCGCAGGGT
CCTGCTGGGCCCTCCCGCCGTGTGGCAGCCAGGACCCTGTGGGCCCCCGGAGAA GACTGAGGAGGAGG
ATGAGGAGGAGGATGGGAGGAGAGCA GGGAGGGGCAAGGGAA GAGATGAACGGCCGGGT CAGCCA
GATCACGCAGCC TGGCACCAGCGGGCAGGAGCGGCCCCAGCAGAGTGGCCAGCAAGGAGCAGCAGCTCCTAC
CCCAA GAGGCTTCCACTGGGAGAAGTCCAGCACGATGGCATCAGCTACCTGGCCGCGAGACGGGAAGCGGAG
CTACTA ACTTCAGCCTGCTGAAGCAGGCTGGCGACGTGAGGAGAAACCCTGGACCTGGTCTCCGGCCGATGGTGA
GCAAGGGCGAGGAGGATTAACATGGCCATCATCAAGGAGTTGATGGCCTTCAAGGTGCACATGGAGGGCTCCGTGAA
CGGCCACGAGTTGAGATCGAGGGCCGAGGGCCGCCCTACGAGGGCACCCAGACC GCCAA GCTGAAGG

TGACCAAGGGTGGCCCCCTGCCCTTGGCTGGGACATCCTGTCCCTCAGTTTCATGTAAGGCTCCAAGGCCCTACGT
GAAGCACCCCGCCGACATCCCCGACTACTGAAGCTGTCTTCCCGGAGGCTTCAAGTGGAGCGCGTGATGAAC
TTGAGGACGGCGGTGGTGAACCGTGACCCAGGACTCCTCCCTGCAGGACGGCGAGTTCATCTACAAGGTGAAG
CTGCGCGCACCAACTTCCCTCCGACGGCCCCGTAATGCAGAAGAAGCCATGGGCTGGAGGCCCTCCTCCGAG
CGGATGTACCCCGAGGACGGCGCCCTGAAGGGCGAGATCAAAGCAGAGGCTGAAAGCTGAAGGACGGCGCCACTAC
GACGCTGAGGTCAAAGACCACCTACAAGGCCAAGAAGCCCGTGCAGCTGCCCGCGCCTACAACGTCAACATCAAGT
TGACATCACCTCCACACAAGAGGACTACACCATCGTGGAACAGTACGAACGGCGCGAGGGCCGCACTCCACCGG
CGGCATGACGAGCTGTACAAGTCCGGAAACTAGTCTCAGATCTCGAGCTCAAGCTTCGAAATTCGCAGTCGACGGT
ACCGGGGGCCGGATCCACCGGATCTAGATACTGATCATATACGCCATACCACATTTGTAGAGGTTTACTTGCT
TTAAAAAACCTCCACACACTCCCCCTGAACCTGAACATAAAAAATGAATGCAATTTGTTGTTAACTTGTTATTGCAG
CTTATAATGGTTACAATAAAGCAATAGCATCACAAATTTACAAAAAAGCAATTTTTTCACTGCATTCTAGTTGTGT
TTGTCCAAACTCATCAATGTATCTTAACGCCGTAATTGTAAGCGTTAATATTTTTGTTAAAAATTCGCGTTAAATTTTTGTTA
AATCAGCTCATTTTTTAACCAATAGCGCAAAATCGCAAAATCCCTATAAATCAAAAAGAAITAGACCGAGATAGGGTTG
AGTGTGTTCCAGTTTGGAACAAGAGTCCACTATTAAAGAAGCGTGACTCCAACGTCAAAAGGGCGAAAAAACCGTCTAT
CAGGGCGATGGCCACTACGTGAACCATCACCCTAATCAAGTTTTTTGGGGTGCAGGTGCCGTAAGCACTAAATCG
GAACCCTAAMAGGGAGGCCCCGATTTAGAGCTTGACGGGGAMAAGCCGGCAACGTGGCGAGAMAAGGAAGGAAAGAA
AGCGAAAAGGAGCGGGCGTAGGGCTGGCAAGTGTAGCGGTCACGCTGCGGGTAACCAACACACCCCGCCGCGCT
TAATGCCCGCTACAGGGCGCGTCAAGGTGGCACTTTTCGGGMAATGTGCGCGGAACCCCTATTTGTTATTTTCT
AAATACATTCAATAITGTATCCGCTCATGAGACAATAACCCGTGATAAATGCTTCAATAATATTGAAAAAGGAAGAGTCC

TGAGCGGAAAGAACCGACTGTGGAATGTGTCAAGTTAGGGTGTGAAAGTCCCAGGCTCCCAGCAGGCAGAA
GTATGCAAAGCATGCATCTCAATTAGTCAGCAACCAGGTGTGMAAGTCCCAGGCTCCCAGCAGGCAGAAATG
CAAAGCATGCATCTCAATTAGTCAGCAACCATAGTCCGCCCTAACTCCGCCCATCCGCCCTAACTCCGCCAG
TTCGCCCATTTCCGCCCATGGCTGACTAATTTTTTATTATGCAGAGGCCGAGGCCCTCGGCTCTGAGCT
ATTCAGAAGTAGTGAGGAGGCTTTTTGGAGGCCTAGGCTTTTGCAAAGATCGATCAAGAGACAGGATGAGGATCG
TTTCGC**ATG**ATTGAACAAGATGGATTGCACGCAAGTTCTCCGGCCGCTTGGGTGGAGAGGCTATTGGCTATGACTG
GGCACAACAGACAATCGGCTGCTCTGATGCCGCCGTGTTCCGGCTGTACGGCAGGGGCCCGGTTCTTTTGTC
AAGACCGACCTGTCCGGTGCCCTGAAATGAACTGCAAGACGAGGCAGCCGGCTATCGTGGCTGGCCACGACGGGC
GTTCCTTGGCGAGCTGTGCTCGACGTTGTCACTGAAAGCGGMAAGGACTGGCTGCTATTGGCCGAAGTGCCGGGG
CAGGATCTCCTGTATCTCACTTGTCTCCTGCCGAGAAAGTATCCATCATGGCTGATGCAATGCCGGCTGCATAC
GCTTGATCCGGCTACCTGCCCATTCGACCACCAAGCGAAACATCGCATCGAGCGAGCAGTACTCGGATGGAAGCC
GGTCTTGTGATCAGGATGATCTGGACGAAGACATCAGGGGCTCGCCAGCCGAACCTGTTCCGACGGCTCAAGG
CGAGCATGCCCGACGGGAGGATCTCGTGTGACCCATGGCGATGCCCTGCTTGCCGAATATCATGGTGGAAAAATGG
CCGCTTTTCTGGATTCA**TG**ACTGTGGCCGGCTGGGTGTGGCCGACCCGCTATCAGGACATAGCGTTGGCTACCCGT
GATATTGCTGAAGAGCTTGGCCGGCGAATGGGCTGACCCGCTTCCTCGTGCCTTACGGTATCGCCGCTCCCGATTGGCA
GGCGATCGCCTTCTATCGCCCTTCTTGACGAGTTCTT**CTGA**CGCGGACTCTGGGTTGMAATGACCGACCAAGCGAC
GCCCAACCTGCCATCACGAGATTTGATTCACCGCCGCTTCTATGAAAAGTTGGGCTTCGGAATCGTTTTCCGGG
ACGCCGGCTGGATGATCCTCCAGCCGGGGATCTCATGTCTGGAGTTCTTCGCCACCCCTAGGGGGAGGCTAACTGA
AACACGGAAGGAGACAATACCGMAAGGAAACCCGCGCTATGACGGCAATAAAAAAGACAGAATAAAAAACGCACCGTGTT

GGGTCGTTTGTTCATAAACGGGGGTTCCGTCGCCAGGGCTGGCACTCTGTGCATACCCACCAGACCCCAATTGGG
GCCAATACGCCCGGTTTCTTCTTTTCCACCACCACCACCAGTTGGGTGAAGGCCCAGGGCTCGCAGCCAA
CGTCGGGGCGGAGGCCCTGCCATAGCCTCAGGTTACTCATATATACTTAGAATTGAITTA AAAACTTCATTTTAATTT
AAAAAGATCTAGGTGAAGATCCTTTTTGATAATCTCATGACCAAAATCCCTTAACGTGAGTTTTCGTTCCACTGAGCGT
CAGACCCCGTAGAAAAGATCAAAGGATCTTCTTGAGATCCTTTTTTCTGCCGTAATCTGCTTGCAAAACAAAAA
ACCACCCTACCAGCGGTGTTTGTGGCCGATCAAGAGCTACCAACTCTTTTCCGAAGGTA ACTGGCTTCAGCA
GAGCGCAGATACCAATACTGTCTCTAGTGTAGCCGTAAGT TAGGCCACCACCTCAAGA ACTCTGTAGCACCCGCT
ACATACCCTCGCTCTGCTAATCCTGTTACCAGTGGCTGCTGCCAGTGGCGATAAGTCTGTCTTACC GGGTTGACTC
AAGACGATAGTTACC GGATAAGCGCAGCGGTCCGGCTGAACGGGGGTTCTGTGCACACAGCCAGCTTGGAGCG
AACGACCTACACCGAACTGAGATACCTACAGCGTGAGCTATGAGAAAAGCCACGCTTCCCGAAAGGGAGAAAAGCGG
GACAGGTATCCGGTAAAGCGGCGAGGGTCCGAAACAGGAGAGCCGACGAGGGAGCTTCCAAGGGGAAACGCCCTGGTAT
CTTTATAGTCTGTGGGTTTCCACCCTCTGACTTGAGCGTCAATTTTTGTGATGCTCGTCAGGGGGCGGAGCCCT
ATGGAAAAACGCCAGCAACGGGCTTTTACGGTTCCTGGCC TTTTGGCTGGCC TTTTGGCTCACA TGTTC TTTCTCTGC
GTTATCCCTGATTCGTGTGATAACCGTATTACC GCCATGCAT

Supplementary Table 1. Affinity profiles of selected ligands of somatostatin receptors.

Ligand	Binding affinity: (IC ₅₀ , nM) / (K _d)*, nM				
	<i>hsSTR 1</i>	<i>hsSTR 2</i>	<i>hsSTR 3</i>	<i>hsSTR 4</i>	<i>hsSTR 5</i>
Somatostatin - 14	1.9 ± 0.5 [13]	5.7 ± 1.1 [18]	3.3 ± 1.2 [19]	1.6 ± 0.8 [13]	15.5 ± 2.6 [18]
	0.7 [14]	0.7 ± 0.2 [19]	3.3 ± 1.7 [13]	1.3 [14]	10 ± 4 [19]
	0.43 ± 0.08 [15]*	0.7 ± 0.2 [13]	0.3 [14]	0.74 ± 0.07 [15]*	4.2 ± 0.7 [13]
	0.4 [16]*	0.2 [14]	0.53 ± 0.21 [15]*	1.7 [16]*	0.5 [14]
	2.0 ± 0.35 [17]*	0.0016 ± 0.0005 [15]*	0.7 [16]*	2.0 ± 0.3 [17]*	0.23 ± 0.04 [15]*
	0.04 [16]*	1.2 ± 0.2 [17]*		2.3 [16]*	
	0.25 ± 0.03 [17]*			1.4 ± 0.3 [17]*	
Somatostatin - 28	3.9 ± 0.3 [20]	2.3 ± 0.1 [19]	3.7 ± 0.3 [19]	3.8 ± 0.3 [20]	2.4 ± 0.2 [19]
	5.2 ± 0.3 [21]	3.3 ± 0.2 [20]	7.1 ± 0.7 [20]	5.6 ± 0.4 [21]	3.9 ± 0.3 [20]
	2.7 ± 0.3 [22]	2.7 ± 0.3 [21]	7.7 ± 0.9 [21]	2.7 ± 0.3 [22]	4.0 ± 0.3 [21]
	2.7 ± 0.2 [23]	2.3 ± 0.2 [22]	3.4 ± 0.3 [22]	2.6 ± 0.4 [23]	2.5 ± 0.3 [22]
	0.6 [14]	2.7 ± 0.2 [23]	3.3 ± 0.4 [23]	7.9 [14]	2.4 ± 0.2 [23]
	1.9 ± 0.4 [17]*	0.3 [14]	5.4 ± 2.5 [17]*	0.4 [14]	
	0.31 ± 0.06 [17]*	0.31 ± 0.06 [17]*	1.3 ± 0.3 [17]*		0.4 ± 0.1 [17]*
Octreotide (SMS-201-995)	> 10,000 [21]	2.0 ± 0.7 [21]	187 ± 55 [21]	> 1000 [21]	22 ± 6 [21]
	290 [14]	1.4 ± 0.3 [18]	5.8 [14]	>1000 [14]	28.9 ± 4.2 [18]
	300 ± 85 [15]*	0.4 [14]	15.2 ± 5.9 [15]*	>1000 [15]*	5.6 [14]

	87.5 [24]*	0.053 ± 0.011 [15]*	26.8 ± 7.7 [24]*	>1000 [24]*	11.5 ± 1.91 [15]*
	>1000 [25]*	0.57 ± 0.06 [24]*	4.4 [25]*	>1000 [25]*	6.78 ± 0.96 [24]*
		2.1 [25]*			5.6 [25]*
[Tyr3]-octreotide	>10 000 [21]**	2.8 ± 0.6 [19]	225 ± 82 [19]	>1000 [21]**	9.9 ± 1.8 [19]
		14 ± 2.6 [21]**	880 ± 324 [21]**		393 ± 84 [21]**
[Tyr3]-octreotate	>10 000 [21]**	1.5 ± 0.4 [21]**	>1000 [21]**	453 ± 176 [21]**	547 ± 160 [21]**
Cyn-154806	> 1000 [26]	3.6 ± 0.4 [26]	> 1000 [26]	349 ± 30 [26]	276 ± 119 [26]
	>1000 [27]	2.6 [27]	>851 [27]	>1000 [27]	331 [27]
	>1000 [28]**#	0.3 [28]**#	100 [28]**#		2.5 [28]**#

The data comes from *in vitro* displacement experiments (competition between a radiolabelled «universal» ligand, most

typically a variant of somatostatin-14 or somatostatin-28, and a non-radioactive peptide in question), performed on

isolated plasma membranes from cells overexpressing defined subtypes of human SSTRs (hSSTR). Mean values ± SEM

(nM) are shown, if not stated otherwise.

* K_i - inhibition constant, nM.

** data for DOTA-chelated (1,4,7,10-Tetraazacyclododecane-1,4,7,10-tetra-acetic acid) compounds is presented.

data for *rat* SSTR subtypes.

IC₅₀ – half-maximal inhibitory concentration, nM.

Supplementary Table 2. Primers employed in the study.

<i>Primer ID#</i>	<i>Primer sequence (5'-3')</i>	<i>Used for</i>	<i>Target amplicon length</i>	<i>Comments</i>
#1	GcgtacgAT <u>Ggattacaag</u> <u>atgatgatgataaag</u> GAGCCC CTGTTCCACGCCCTCCA C	Amplification and cloning of <i>SSTR5</i> wild-type (WT) coding sequence from human gDNA	1129 bp (#1+2 as a pair)	Includes a recognition site for BsiWI (small bold letters), the initiation codon (BOLD CAPITAL LETTERS) and a sequence for FLAG-tag (<i>small italic underlined letters</i>).
#2	gcgcgcc CAGCTTGCTG GTCTGCATAAGCC	Amplification and cloning of <i>SSTR5</i> WT coding sequence from human gDNA	1129 bp (#1+2 as a pair)	Includes a recognition site for BssHII (small bold letters).
#3	TAATACGACTCACTAT AGGG	PCR screen and sequencing of inserts ligated into pCDNA 3.1/V5-His TOPO-TA vector	267 bp + the length of insert (#3+4 as a pair)	In the absence of insert the vector remains open and does not support PCR amplification (no product).
#4	CTAGAAGGCACAGTC GAGGC	PCR screen and sequencing of inserts ligated into pCDNA 3.1/V5-His TOPO-TA vector	267 bp + the length of insert (#3+4 as a pair)	In the absence of insert the vector remains open and does not support PCR amplification (no product).
#5	CGGTTTGACTCACGG GGAT	PCR screen and sequencing of inserts ligated into AmCyan-P2A-mCherry	341 bp + the length of insert (#5+6 as a pair)	In the absence of insert BsmBI-linearized vector remains open and does not support PCR amplification (no product). The

		vector		original non-digested vector should give a product of 1141 bp upon PCR.
#6	GCGCATGAACCTCTTG ATGA	PCR screen and sequencing of inserts ligated into AmCyan-P2A-mCherry vector	341 bp + the length of insert (#5+6 as a pair)	In the absence of insert BsmBI-linearized vector remains open and does not support PCR amplification (no product).
#7	ACCTGCCAACCAAGC GAGAAC	PCR screen and sequencing of inserts ligated into pMiniT vector	246 bp + the length of insert (#7+8 as a pair)	In the absence of insert the vector remains open and does not support PCR amplification (no product).
#8	TCAGGGTTATTGTCTC ATGAGCG	PCR screen and sequencing of inserts ligated into pMiniT vector	246 bp + the length of insert (#7+8 as a pair)	In the absence of insert the vector remains open and does not support PCR amplification (no product).
#9	<u>AACCGTCAGATCCCGT</u> <u>CTCCCGTACGATGTAC</u> CCATACGATG	Preparation of SSTR2HA coding sequence for ligation into AmCyan-P2A-mCherry plasmid by means of Gibson assembly	1180 bp (#9+10 as a pair)	The primer introduces a 20-nucleotide overhang to the 5-prime of the amplicon, which is complementary to the left arm of the linearized hosting vector <u>(CAPITAL ITALIC UNDERLINED LETTERS).</u>
#10	<u>AAGTTAGTAGCTCCGC</u>	Preparation of SSTR2HA	1180 bp	The primer introduces a 20-nucleotide

	<u>TTCGATACTGGTTTG</u> GAGGTCTC	coding sequence for ligation into AmCyan-P2A-mCherry plasmid by means of Gibson assembly	(#9+10 as a pair)	overhang to the 3-prime of the amplicon, which is complementary to the right arm of the linearized hosting vector (<u>CAPITAL ITALIC UNDERLINED LETTERS</u>).
#11	GcgtaccgATG <u>ta</u> cccaatccg <u>atgttc</u> cagattaccgcGACAT GGCCGATGAGCCACT CAA	Amplification and cloning of SSTR2 WT coding sequence from human gDNA	1147 bp (#11+12 as a pair)	Includes a recognition site for BsiWI (small bold letters), the initiation codon (BOLD CAPITAL LETTERS) and a sequence for HA-tag (<i>small italic underlined letters</i>)
#12	gcg cgcgGATACTGGTTT GGAGGTCTCCAT	Amplification and cloning of SSTR2 WT coding sequence from human gDNA	1147 bp (#11+12 as a pair)	Includes a recognition site for BssHII (small bold letters)
#13	GcgtaccgATG <u>ga</u> acaataaa <u>ctcatc</u> cagaagaagatctgG ACATGCTTCATCCATC ATCGGT	Amplification and cloning of SSTR3 WT coding sequence from human gDNA	1297 bp (#13+14 as a pair)	Includes a recognition site for BsiWI (small bold letters), the initiation codon (BOLD CAPITAL LETTERS) and a sequence for Myc-tag (<i>small italic underlined letters</i>)
#14	gcg cgcgCCAGGTAAGCTG ATGCCGATCGTGC	Amplification and cloning of SSTR3 WT coding sequence from human gDNA	1297 bp (#13+14 as a pair)	Includes a recognition site for BssHII (small bold letters)

REFERENCES

1. Pfeiffer M, Koch T, Schröder H, Klutzny M, Kirscht S, Kreienkamp HJ, Höllt V, Schulz S. Homo- and heterodimerization of somatostatin receptor subtypes. Inactivation of sst(3) receptor function by heterodimerization with sst(2A). *J Biol Chem*. 2001 Apr 27;276(17):14027–36.
2. Liu Q. Receptor signaling and endocytosis are differentially regulated by somatostatin analogs. *Mol Pharmacol*. 2005 Apr 25;68(1):90–101.
3. Lesche S, Lehmann D, Nagel F, Schmid H a, Schulz S. Differential effects of octreotide and pasireotide on somatostatin receptor internalization and trafficking in vitro. *J Clin Endocrinol Metab*. 2009 Feb;94(2):654–61.
4. Szymczak-Workman AL, Vignali KM, Vignali DAA. Design and construction of 2A peptide-linked multicistronic vectors. *Cold Spring Harb Protoc*. 2012;7(2):199–204.
5. Reubi JC, Schonbrunn A. Illuminating somatostatin analog action at neuroendocrine tumor receptors. *Trends Pharmacol Sci*. 2013 Dec;34(12):676–88.
6. Huang RD, Smith MF, Zahler WL. Inhibition of forskolin-activated adenylate cyclase by ethanol and other solvents. *J Cyclic Nucleotide Res*. 1982;8(6):385–94.
7. Robberecht P, Waelbroeck M, Chatelain P, Jean-Claude C, Jean C. Inhibition of Forskolin-stimulated cardiac adenylate cyclase activity by short-chain alcohols. *FEBS Lett*. 1983;154(1):205–8.
8. Stenstrom S, Seppala M, Pfenning M, Richelson E. Inhibition by ethanol of forskolin-stimulated adenylate cyclase in a murine neuroblastoma clone (N1E-115). *Biochem Pharmacol*. 1985 Oct;34(20):3655–9.

9. Bode DC, Molinoff PB. Effects of ethanol in vitro on the beta adrenergic receptor-coupled adenylate cyclase system. *J Pharmacol Exp Ther.* 1988 Sep;246(3):1040–7.
10. Kelly E, Harrison PK, Williams RJ. Effects of acute and chronic ethanol on cyclic AMP accumulation in NG108-15 cells: differential dependence of changes on extracellular adenosine. *Br J Pharmacol.* 1995 Apr;114(7):1433–41.
11. Diamond I, Gordon AS. Cellular and molecular neuroscience of alcoholism. *Physiol Rev.* 1997;77(1):1–20.
12. Terama E, Ollila OHS, Salonen E, Rowat AC, Trandum C, Westh P, Patra M, Karttunen M, Vattulainen I. Influence of ethanol on lipid membranes: From lateral pressure profiles to dynamics and partitioning. *J Phys Chem B.* 2008;112(13):4131–9.
13. Tatsi A, Maina T, Cescato R, Waser B, Krenning EP, de Jong M, Cordopatis P, Reubi J-C, Nock BA. [DOTA]Somatostatin-14 analogs and their ¹¹¹In-radioligands: Effects of decreasing ring-size on sst1–5 profile, stability and tumor targeting. *Eur J Med Chem.* 2014;73:30–7.
14. Bruns C, Raulf F, Hoyer D, Schloos J, Lübbert H, Weckbecker G. Binding properties of somatostatin receptor subtypes. *Metabolism.* 1996 Aug;45(8 Suppl 1):17–20.
15. Ramón R, Martín-Gago P, Verdaguer X, Macias MJ, Martín-Malpartida P, Fernández-Carneado J, Gomez-Caminals M, Ponsati B, López-Ruiz P, Cortés MA, Colás B, Riera A. SSTR1- and SSTR3-selective somatostatin analogues. *Chembiochem.* 2011 Mar 7;12(4):625–32.
16. Rohrer SP. Rapid Identification of Subtype-Selective Agonists of the Somatostatin Receptor Through Combinatorial Chemistry. *Science (80-).* 1998;282(5389):737–40.
17. Rajeswaran WG, Hocart SJ, Murphy WA, Taylor JE, Coy DH. Highly potent and subtype

- selective ligands derived by N-methyl scan of a somatostatin antagonist. *J Med Chem.* 2001;44(8):1305–11.
18. Kliewer A, Mann A, Petrich A, Pöll F, Schulz S. A transplantable phosphorylation probe for direct assessment of G protein-coupled receptor activation. *PLoS One.* 2012 Jan;7(6):e39458.
 19. Cescato R, Schulz S, Waser B, Eltschinger V, Rivier JE, Wester H-J, Culler M, Ginj M, Liu Q, Schonbrunn A, Reubi JC. Internalization of sst2, sst3, and sst5 receptors: effects of somatostatin agonists and antagonists. *J Nucl Med.* 2006 Mar;47(3):502–11.
 20. Reubi JC, Schaer JC, Wenger S, Hoeger C, Erchegyi J, Waser B, Rivier J. SST3-selective potent peptidic somatostatin receptor antagonists. *Proc Natl Acad Sci U S A.* 2000 Dec 5;97(25):13973–8.
 21. Reubi JC, Schär JC, Waser B, Wenger S, Heppeler A, Schmitt JS, Mäcke HR. Affinity profiles for human somatostatin receptor subtypes SST1-SST5 of somatostatin radiotracers selected for scintigraphic and radiotherapeutic use. *Eur J Nucl Med.* 2000 Mar;27(3):273–82.
 22. Ginj M, Zhang H, Eisenwiener K-P, Wild D, Schulz S, Rink H, Cescato R, Reubi JC, Maecke HR. New pansomatostatin ligands and their chelated versions: affinity profile, agonist activity, internalization, and tumor targeting. *Clin Cancer Res.* 2008 Apr 1;14(7):2019–27.
 23. Cescato R, Erchegyi J, Waser B, Piccand V, Maecke HR, Rivier JE, Reubi JC. Design and in vitro characterization of highly sst2-selective somatostatin antagonists suitable for radiotargeting. *J Med Chem.* 2008;51(13):4030–7.
 24. Rueter JK, Mattern R, Zhang L, Taylor J, Morgan B, Hoyer D, Goodman M. Syntheses and biological activities of sandostatin analogs containing stereochemical changes in positions 6 or 8. *Biopolymers.* 2000 May;53(6):497–505.

25. Patel YC, Srikant CB. Subtype selectivity of peptide analogs for all five cloned human somatostatin receptors (hsstr 1-5). *Endocrinology*. 1994 Dec;135(6):2814–7.
26. Ginj M, Zhang H, Waser B, Cescato R, Wild D, Wang X, Erchegyi J, Rivier J, Mäcke HR, Reubi JC. Radiolabeled somatostatin receptor antagonists are preferable to agonists for in vivo peptide receptor targeting of tumors. *Proc Natl Acad Sci U S A*. 2006 Oct 31;103(44):16436–41.
27. Feniuk W, Jarvie E, Luo J, Humphrey PPA. Selective somatostatin sst2 receptor blockade with the novel cyclic octapeptide, CYN-154806. *Neuropharmacology*. 2000;39(8):1443–50.
28. Bass RT, Buckwalter BL, Patel BP, Pausch MH, Price LA, Strnad J, Hadcock JR. Identification and characterization of novel somatostatin antagonists. *Mol Pharmacol*. 1996 Oct;50(4):709–15.